On the effects of numerical parameters for vortex-induced vibration of a circular cylinder

Y. H. Irawan, *Department of Mechanical Engineering, National Taiwan University of Science and Technology* (d10803806@mail.ntust.edu.tw)
Advisor: Prof. Ming-Jyh Chern

Abstract

A direct-forcing immersed boundary (DFIB) method is used in an in-house parallelized C++ code to simulate the VIV responses for an elastically mounted circular cylinder in the laminar and turbulent flow regimes. The continuity and Navier-Stokes equations are solved together with the equation of motion to capture the VIV phenomenon. The speedup of the solver using OpenMP parallelization is calculated. The VIV responses for detailed grid independence studies in both laminar and turbulent flows are discussed. The importance of conducting grid independence study inside the lock-in region for VIV simulations has been ascertained through detailed comparisons of coarser and finer grids in each of the flow regimes. For laminar flows, the effect of the grid on evolution of the vibration response is investigated. For turbulent flows, the effect of different initial conditions on the VIV amplitude is studied and hysteresis phenomena is observed in the initial and upper branches.

Keywords: vortex-induced vibration, direct-forcing immersed boundary method, grid independence study, elastically mounted circular cylinder.

Introduction

The presence of blunt body (e.g. circular cylinder) in the fluid flow results in generation of vortices behind the body with an alternating pattern, which also produce alternating forces. Once the frequency of those vortices/forces is close enough to the structure's natural frequency, the body starts to oscillate rapidly and enters into lock-in condition. This is also known as vortex-induced vibration (VIV).

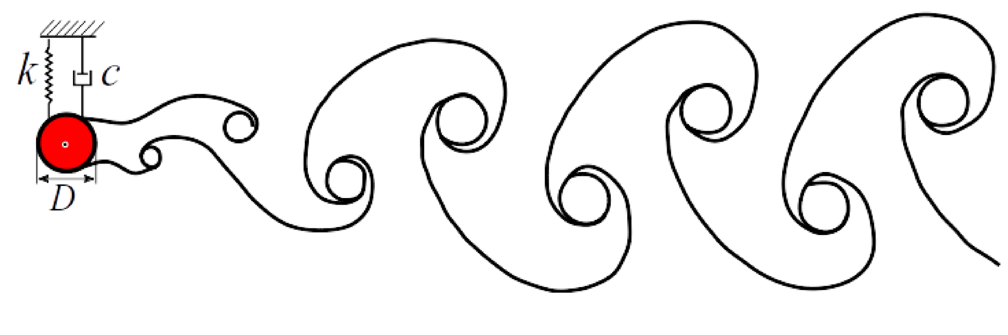

Figure 1. VIV phenomenon

This phenomenon can damage the engineering structure and should be avoided as much as possible. VIV can also be used as renewable energy by using its alternating motion. VIVACE is a type of device for harvesting energy using the VIV phenomenon. The focus of this study is to investigate the VIV phenomenon numerically in three-dimensional fluid flow for the laminar and turbulent flow regimes.

Problem description

One way to verify numerical results is to perform a grid independence study. The grid independence study checks the effect of the grid on the accuracy of the solution. Usually, the grid independence study is carried out by taking a set of simulation parameters and calculating them with different grid sizes until the optimal grid size is obtained.

The present study highlights the importance of conducting grid independence study inside the lock-in region for VIV simulations. A direct-forcing immersed boundary (DFIB) method is used to simulate the VIV responses for an elastically mounted circular cylinder in laminar and turbulent flow regimes. An in-house C++ code based on finite volume method has been used. To speed up the calculation process, OpenMP is employed to perform parallel computations. The details of simulation parameters are presented in table 1 and figure 2.

Table 1. Simulation parameters

Parameter	Laminar case	Turbulent case
U_R^*	5.0 – 6.4	0.5 - 10
m^*	149.1	2.0
ζ	0.0012	0.0
Re	90 - 115	1,000

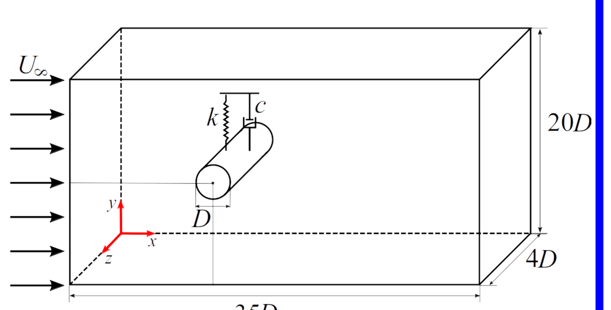

Figure 2. Computational domain

Numerical method

The non-dimensional continuity and Navier-Stokes equations for an incompressible flow are solved using the projection method.

$$\nabla \cdot \mathbf{u} = 0$$

$$\frac{\partial \mathbf{u}}{\partial t} + \nabla \cdot (\mathbf{u}\mathbf{u}) = -\nabla p + \frac{1}{\mathrm{Re}}\nabla^2 \mathbf{u} + \eta \boldsymbol{f}$$

The numerical procedures are explained in the following steps.

1. Identify solid structure using volume of solid function (η).
2. Compute the first intermediate velocity **u*** by just solving the diffusive and convective parts of Navier-Stokes equation.
$$\frac{\mathbf{u}^* - \mathbf{u}^n}{\Delta t} = -\nabla \cdot (\mathbf{u}\mathbf{u}) + \frac{1}{\mathrm{Re}}\nabla^2 \mathbf{u}$$
3. Solve the pressure Poisson equation and then advance to the second intermediate velocity **u****.
$$\frac{\mathbf{u}^{**} - \mathbf{u}^*}{\Delta t} = -\nabla p^{n+1}$$
4. Solve for the virtual force and calculate the total force acting on the solid.
$$\eta \boldsymbol{f} = \frac{\mathbf{u}^{n+1} - \mathbf{u}^{**}}{\Delta t}$$
5. Solve the VIV equation to get structure velocity and structure position.
$$\ddot{Y} + \frac{4\pi\zeta}{U_R^*}\dot{Y} + \left(\frac{2\pi}{U_R^*}\right)^2 Y = \frac{2C_l(t^*)}{\pi m^*}$$

Smagorinsky model has been used in this study with Smagorinsky constant, Cs = 0.1, for all of the turbulent flow simulations.

Results and discussion

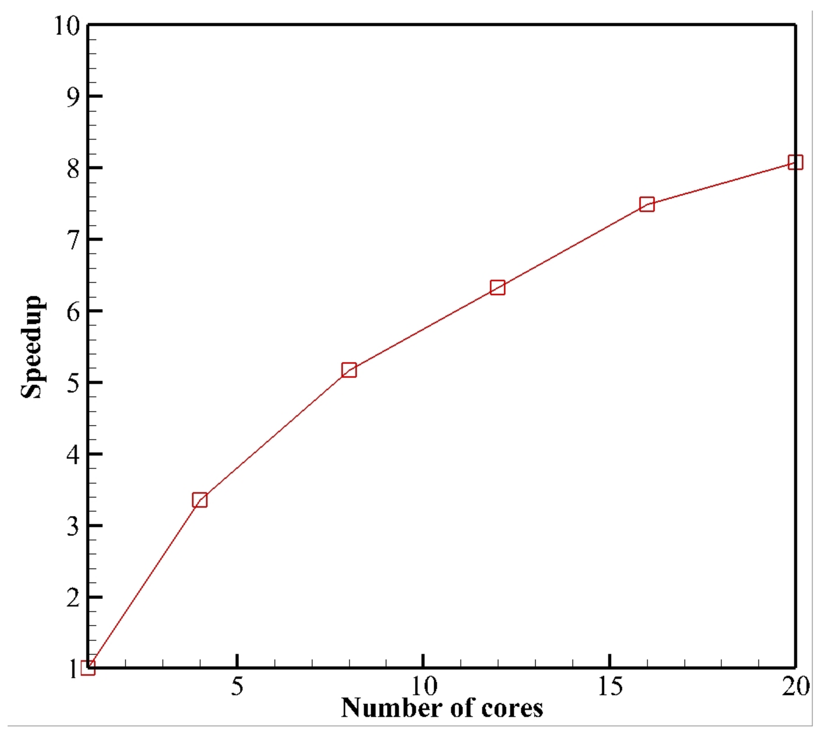

Figure 3. Performance of parallel computations using OpenMP.

Our in-house C++ code provides an eight times speedup over the serial (single-core) computation for a typical problem of flow over a cylinder. Performance tests were conducted on machines with Intel® Xeon® Processor E5-2640 v4.

Although a coarser grid for laminar and turbulent flow cases can satisfy the grid independence requirements for some reduced velocities outside the lock-in region, further grid refinement leads to improved results in the lock-in region where the vibration amplitude increases significantly.

Another VIV phenomenon that can be observed is hysteresis where the structure produces different responses when modeled by increasing and decreasing reduced velocity initial conditions.

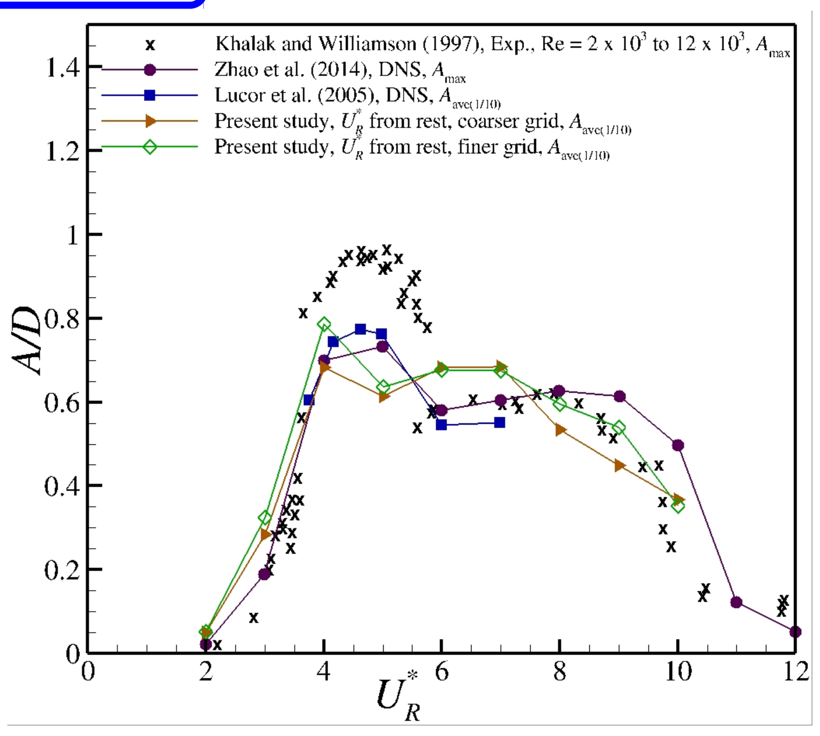

Figure 8. VIV vibration amplitudes for turbulent regime (U_R^* from rest).

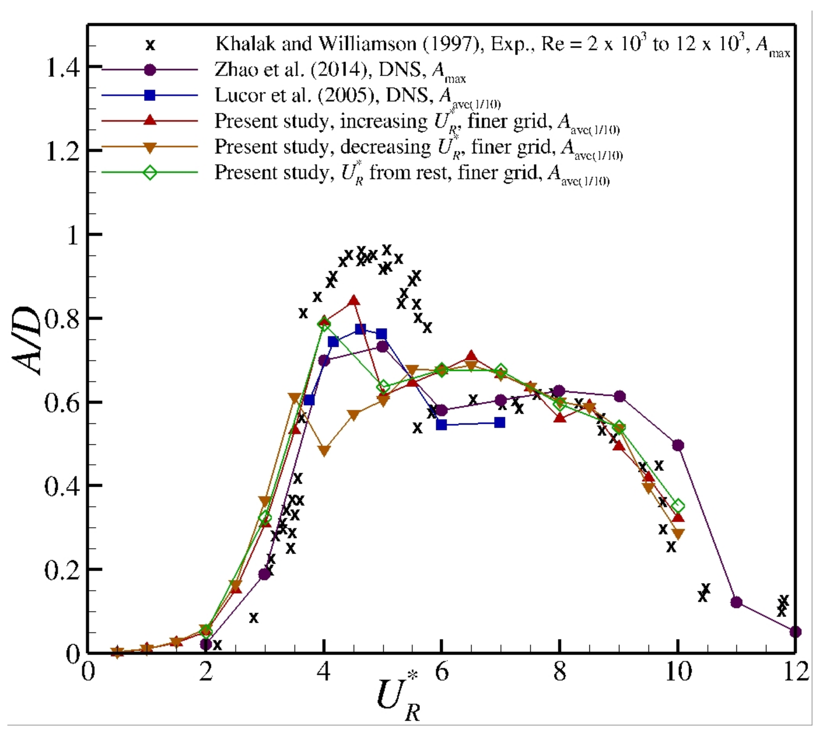

Figure 9. VIV vibration amplitudes for turbulent regime U_R^* from rest, increasing U_R^*, and decreasing U_R^*).

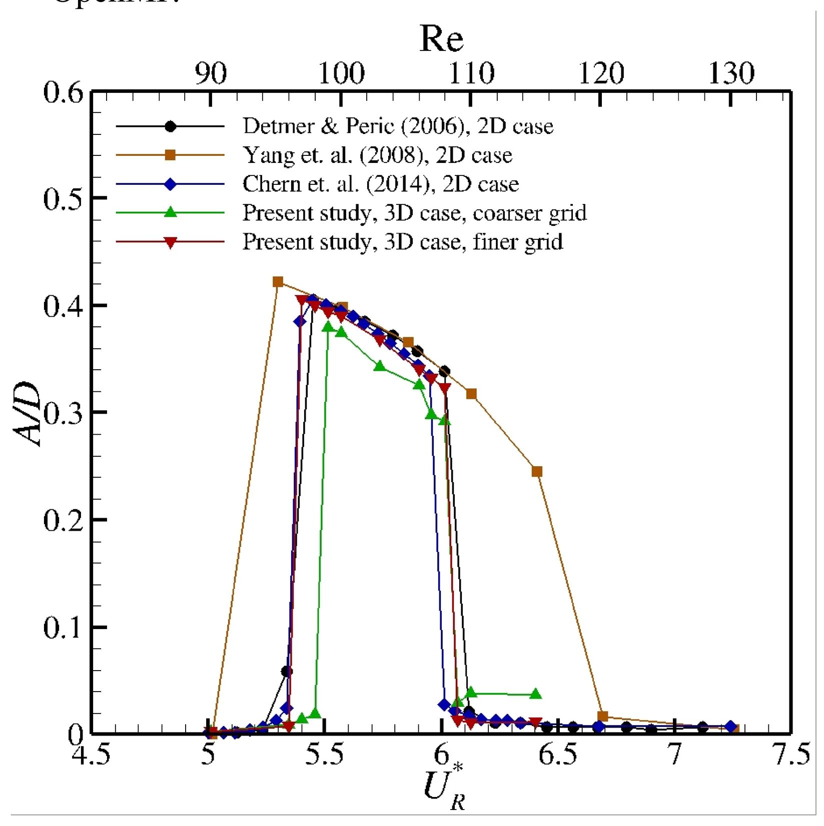

Figure 4. VIV vibration amplitudes for laminar regime.

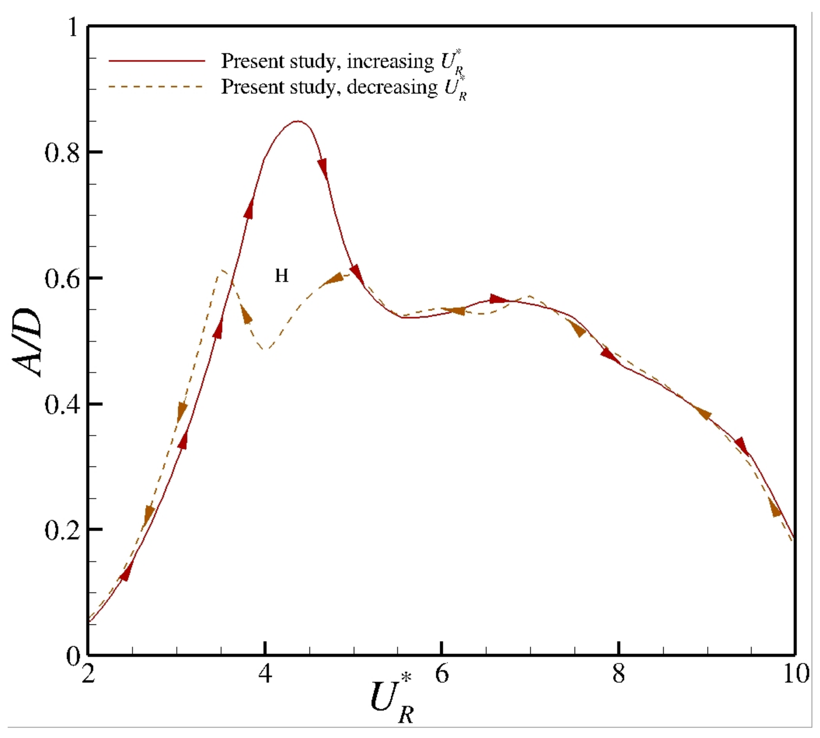

Figure 5. Hysteresis phenomena for turbulent regime.

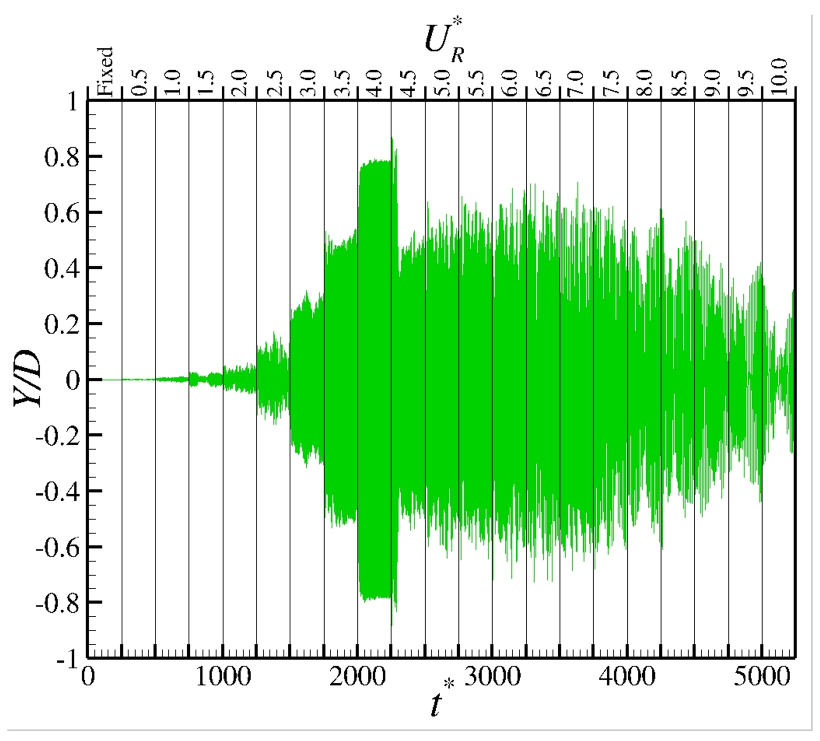

Figure 10. Time history data for turbulent case using increasing U_R^*.

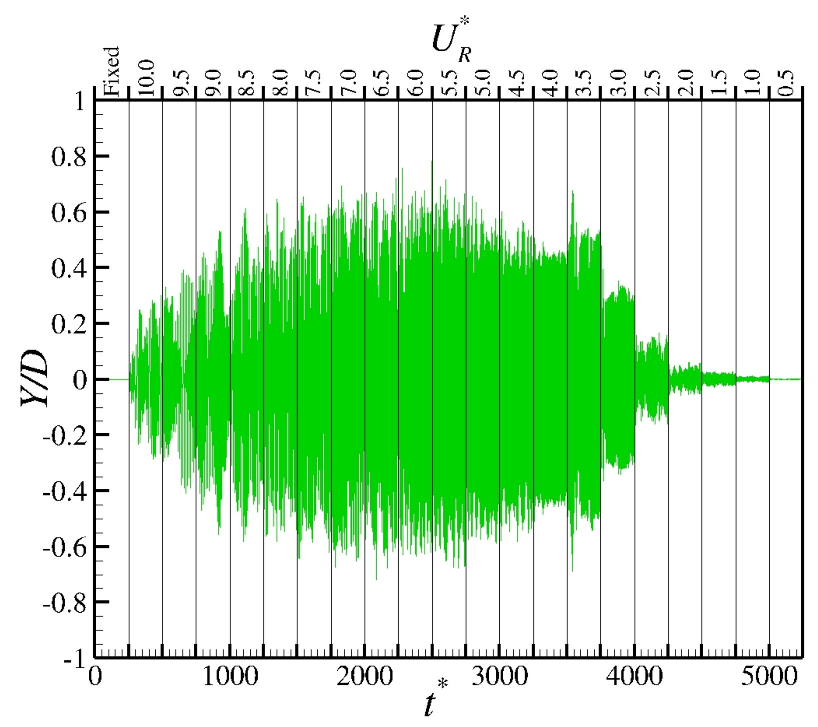

Figure 11. Time history data for turbulent case using decreasing U_R^*.

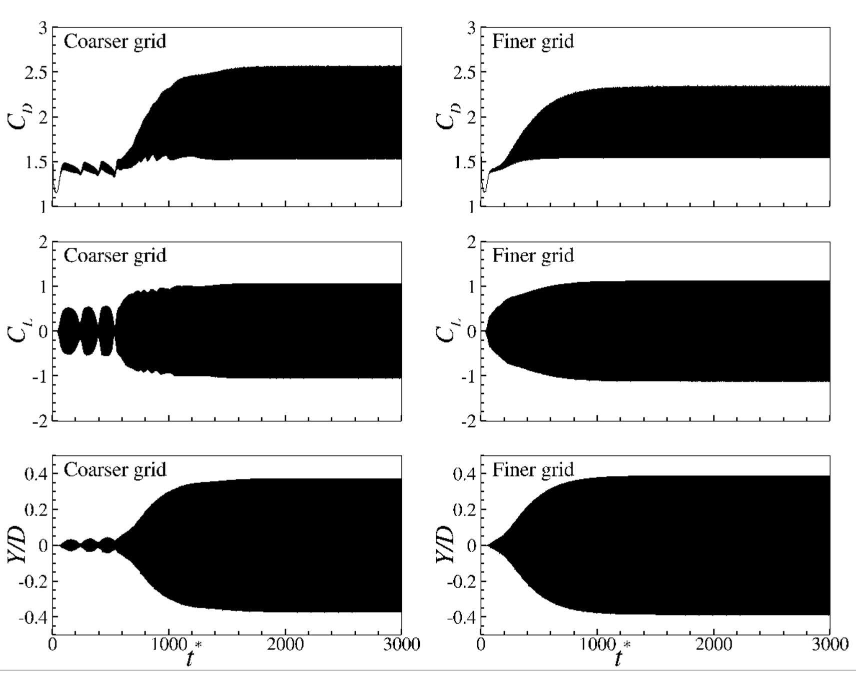

Figure 6. Time history data for laminar case at Re = 100.

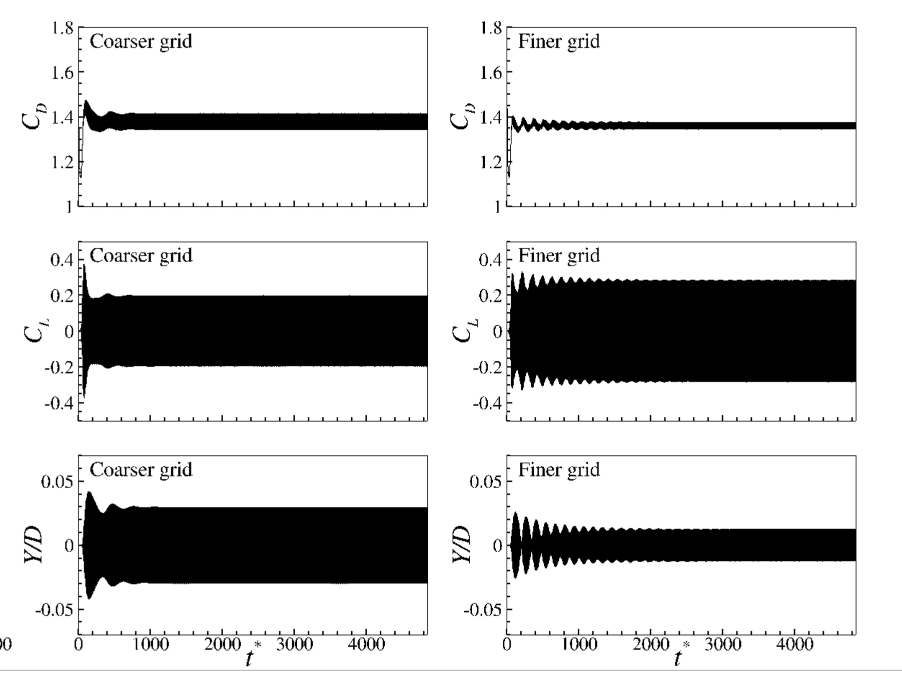

Figure 7. Time history data for laminar case at Re = 109.

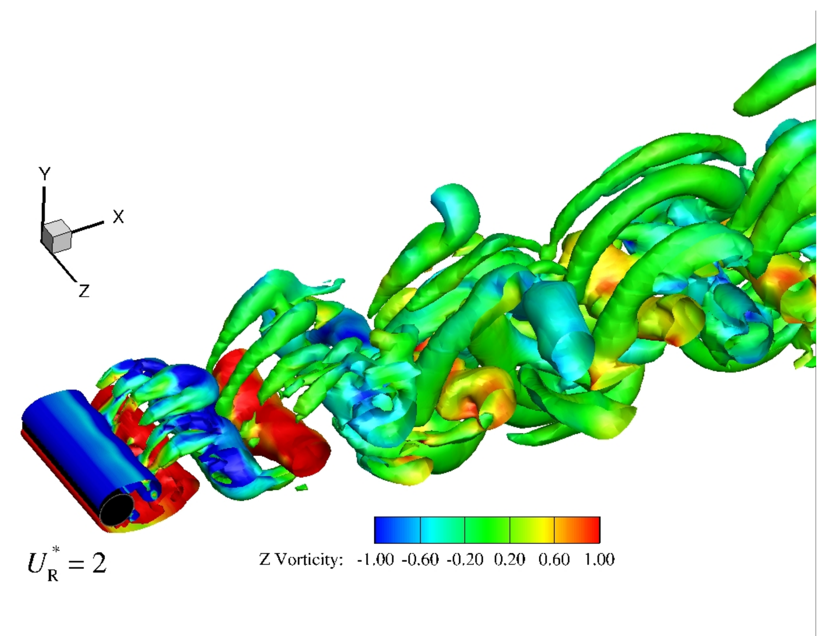

Figure 12. Instantaneous flow structures visualized using Q-criterion at $U_R^* = 2$ (increasing U_R^*).

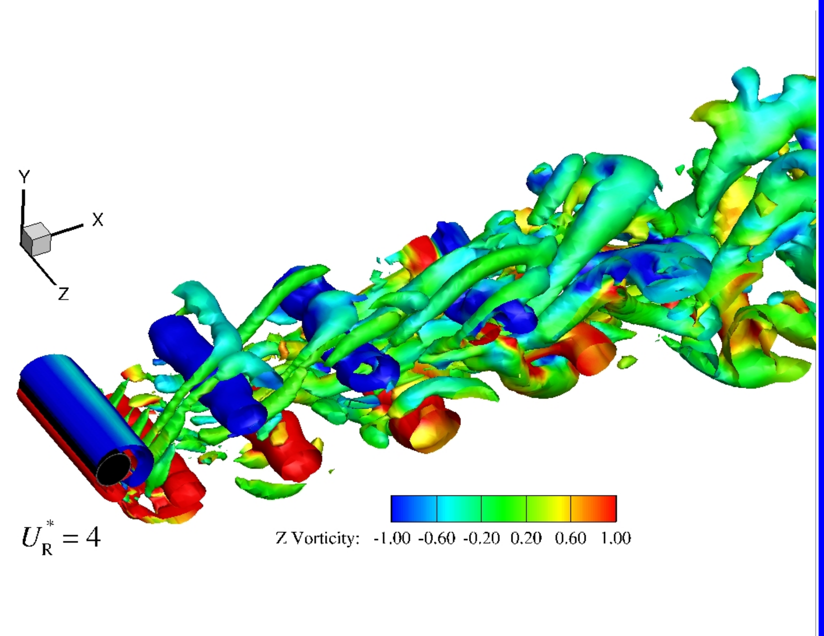

Figure 13. Instantaneous flow structures visualized using Q-criterion at $U_R^* = 4$ (increasing U_R^*).

Conclusions

1. For numerical studies involving VIV phenomenon, the grid independence study should be conducted inside the lock-in region for laminar and turbulent flow regimes.
2. For laminar flows in the lock-in region, the grid refinement not only improves prediction of the VIV amplitude but also affects the evolution of vibration to a stable pattern.
3. In turbulent flows with VIV, switching the initial condition from increasing U_R^* to decreasing U_R^* leads to hysteresis phenomena in the initial and upper branches of the lock-in region.

Acknowledgments

The authors acknowledge the financial support from Ministry of Science and Technology, Taiwan (grant no. MOST-107-2221-E-011-075-MY3). Some of the calculations were carried out on the National Center for High-Performance Computing (NCHC), Taiwan.

References

1. A. Khalak and C. H. K. Williamson, "Fluid forces and dynamics of a hydroelastic structure with very low mass and damping," Journal of Fluids and Structures, vol. 11, no. 8, pp. 973–982, 1997.
2. D. Lucor, J. Foo, and G. E. Karniadakis, "Vortex mode selection of a rigid cylinder subject to VIV at low mass-damping," Journal of Fluids and Structures, vol. 20, no. 4 SPEC. ISS., pp. 483–503, 2005.
3. Dettmer and D. Perić, "A computational framework for fluid-rigid body interaction: Finite element formulation and applications," Computer Methods in Applied Mechanics and Engineering, vol. 195, no. 13–16, pp. 1633–1666, 2006.
4. J. Yang, S. Preidikman, and E. Balaras, "A strongly coupled, embedded-boundary method for fluid-structure interactions of elastically mounted rigid bodies," Journal of Fluids and Structures, vol. 24, no. 2, pp. 167–182, 2008.
5. M. Zhao, L. Cheng, H. An, and L. Lu, "Three-dimensional numerical simulation of vortex-induced vibration of an elastically mounted rigid circular cylinder in steady current," Journal of Fluids and Structures, vol. 50, pp. 292–311, 2014.
6. M. J. Chern, Y. H. Kuan, G. Nugroho, G. T. Lu, and T. L. Horng, "Direct-forcing immersed boundary modeling of vortex-induced vibration of a circular cylinder," Journal of Wind Engineering and Industrial Aerodynamics, vol. 134, pp. 109–121, 2014.